Journal of Computational Physics 281 (2015) 135–147

Contents lists available at ScienceDirect

Journal of Computational Physics

www.elsevier.com/locate/jcp

Volume-preserving algorithms for charged particle dynamics

Yang He [b], Yajuan Sun [a,*], Jian Liu [b], Hong Qin [b,c]

[a] LSEC, Academy of Mathematics and Systems Science, Chinese Academy of Sciences, P.O. Box 2719, Beijing 100190, China
[b] Department of Modern Physics and Collaborative Innovation Center for Advanced Fusion Energy and Plasma Sciences, University of Science and Technology of China, Hefei, Anhui 230026, China
[c] Plasma Physics Laboratory, Princeton University, Princeton, NJ 08543, USA

ARTICLE INFO

Article history:
Received 22 October 2013
Received in revised form 19 September 2014
Accepted 15 October 2014
Available online 22 October 2014

Keywords:
Lorentz force equation
Splitting method
Volume-preserving integrator
Boris algorithm
Conservative quantities

ABSTRACT

The paper reports the development of volume-preserving algorithms using the splitting technique for charged particle motion under the Lorentz force. The source-free nature of the Lorentz vector field has been investigated. Based on the volume-preserving property of the dynamics, a class of numerical methods for advancing charged particles in a general electromagnetic field has been constructed by splitting the classical evolution operator. This new class of numerical methods, which includes the Boris algorithm as a special case, conserves phase space volume, and globally bounds the numerical errors of energy, momentum, and other adiabatic invariants up to the order of the method over a very long simulation time. These algorithms can be computed explicitly, and thus are effective for the long-term simulation of the multi-scale dynamics of plasmas.

1. Introduction

Plasma [1] is a collection of charged particles interacting with electromagnetic fields, whose sources can be either external or internal to the plasma. In the collective dynamics of magnetized plasmas, the most fundamental physical process is the motion of charged particles under the influence of electromagnetic fields. Many important phenomena in plasmas can be understood and analyzed in terms of the single-particle motion which satisfies the Lorentz force equations. Development of efficient computation methods for the single particle model will greatly facilitate the study of the dynamic behavior of plasmas.

In the study of the single particle motion and the guiding center dynamics [2], the (variational) symplectic methods, which have been developed in [3,4], often capture the nature of the physical process better in terms of preserving the phase space structure, while globally bounding the numerical errors of conserved quantities, such as the energy. This can be explained in the framework of the so-called geometric integration. Geometric integrators or structure-preserving methods are numerical methods that inherit the intrinsic geometric properties of the given dynamical system. This class of numerical methods often exhibits superior properties in long time numerical simulation over traditional methods. Specifically, it has been proved theoretically that for Hamiltonian systems the errors of quasi-periodic solutions computed by symplectic integrators have the long-term linear growth [5,6]. Classified by geometric properties of numerical methods, typical geometric numerical methods include symplectic methods for Hamiltonian systems, invariant-preserving methods for systems with constants of motion, volume-preserving methods for source-free systems, etc.

* Corresponding author.
E-mail address: sunyj@lsec.cc.ac.cn (Y. Sun).

http://dx.doi.org/10.1016/j.jcp.2014.10.032
0021-9991/

The motion of charged particles in single particle model is governed by the Newton equation under the Lorentz force exerted by a given electromagnetic field. Hamiltonian formulation is available for the single particle model and other magnetized plasma models in special coordinates [7,8]. Unfortunately, in terms of the canonical variables $(\mathbf{x}, \mathbf{p})$ the resulting equation of motion cannot be separated, and symplectic methods are usually implicit and rather cumbersome to implement. The Lorenz force system can also be written in $(\mathbf{x}, \mathbf{v})$ with $\mathbf{x}$ being the position variables and $\mathbf{v}$ being the velocity variables. In the coordinates $(\mathbf{x}, \mathbf{v})$ the Lorenz force system has, generally, a non-canonical structure, but constructing numerical methods that can preserve the structure is not easy.

In simulating the motion of charged particles, the popular explicit integrators include the fourth order Runge–Kutta method (*RK*4) [9] and the Boris method [10,11]. Though *RK*4 can have a small numerical error at each time step, the numerical errors will accumulate coherently, and become significantly large over many time steps. In contrast, the Boris method, though is only of the second order, shows a good long-term accuracy, and has been successfully applied in simulation studies of magnetized plasmas over forty years. The idea of the Boris method is to alternate position advance with acceleration, and the acceleration is decomposed as an electric acceleration at half step, a rotation caused by the magnetic field at one step and an electric acceleration at half step. Thus it can be computed explicitly. The Boris scheme is time-symmetric (see p. 42 of [9] for definition), and shows excellent conservative properties which was only confirmed numerically [12]. Qin et al. recently have proved that even though the Boris method cannot be canonical or non-canonical symplectic, it is actually volume-preserving [13]. The structural property of the Boris scheme, in some sense, guarantees its good behavior in electromagnetic particle-in-cell simulations. Stimulated by this idea, our purpose of this paper is to construct a class of numerical methods which is explicit and conserves the phase space volume for the Lorenz force system.

The general methods of constructing volume-preserving methods include the generating function approach [14,15] and the splitting approach [16,17]. As the numerical methods based on generating functions are usually implicit, in the present study we choose to design volume-preserving numerical methods based on the splitting technique. The splitting technique [18] is applicable when the evolution vector field can be split into a sum of two or more components, each of which is simpler to solve than the original system. It has been widely applied in research fields like fluid dynamics, celestial mechanics, quantum statistical mechanics, and plasma physics [19,20]. The integrators derived with the splitting technique can be high order and easy to compute. More importantly, when each component of the evolution vector fields belongs to the same Lie subalgebra $L \subset V$, where V is the Lie algebra defined by all the vector fields in the phase space with a Lie bracket, the resulting integrator is geometry-preserving if each subsystem is solved exactly or approximately by a corresponding geometric numerical method (see [16] for more details). This provides a very general and flexible approach of constructing geometric numerical integrators. Splitting methods have been successfully applied to construct the symplectic and energy-preserving methods for simulating the charged particles in electromagnetic fields (see [21,22]). Specifically, for the static and homogeneous magnetic field the so-called Cyclotronic integrator with good accuracy has been developed [23].

In this paper, we study the geometric properties of the Lorenz force system in the $(\mathbf{x}, \mathbf{v})$ coordinates. It is known that the solution of this system can preserve the volume in phase space, as well as the energy, and the magnetic moment if the magnetic field changes slowly with respect to space and time. Based on this property we design a class of splitting methods which is explicit and ensures the conservation of the phase space volume. Moreover, the popular Boris algorithm can be recovered as a special case in this setting. We investigate the long-term conservative properties of the new class of algorithms, and show numerically that the numerical errors on conservative quantities can be bounded up to the order of the method over long-time.

The outline of this paper is as follows. In the next section, we review different formulations of the dynamics of charged particles in the electromagnetic field. We also analyze the corresponding geometric and conservative properties. In Section 3, we show that the motion equation can be split as three subsystems, each of which can be solved exactly. Based on the splitting technique, then we present a class of volume-preserving numerical methods which has high order of accuracy. In Section 4, numerical experiments are presented. Section 5 concludes this paper.

2. The motion equation under Lorentz force

For a charged particle in the electromagnetic field, its dynamics is governed by the Newton–Lorentz equation

$$m\ddot{\mathbf{x}} = q(\mathbf{E} + \dot{\mathbf{x}} \times \mathbf{B}), \quad \mathbf{x} \in \mathbb{R}^3, \tag{1}$$

where $\mathbf{x}$ is the position of the charged particle, m is the mass, and q denotes the electric charge. For convenience, here we assume that $\mathbf{B}$ and $\mathbf{E}$ are static, thus $\mathbf{B} = \nabla \times \mathbf{A}$ and $\mathbf{E} = -\nabla\varphi$ with $\mathbf{A}$ and φ the potentials.

Let the conjugate momentum be $\mathbf{p} = m\dot{\mathbf{x}} + q\mathbf{A}(\mathbf{x})$, then the system (1) is Hamiltonian with

$$H(\mathbf{x}, \mathbf{p}) = \frac{1}{2m}\big(\mathbf{p} - q\mathbf{A}(\mathbf{x})\big) \cdot \big(\mathbf{p} - q\mathbf{A}(\mathbf{x})\big) + q\varphi(\mathbf{x}), \tag{2}$$

which enables the use of canonical symplectic algorithms. However, for this system the general symplectic Runge–Kutta methods (even the methods by the splitting technique) cannot be explicit [6,21,22], because the Hamiltonian (2) is not separable, that is, it cannot be split into the form $H(\mathbf{x}, \mathbf{p}) = T(\mathbf{p}) + V(\mathbf{x})$.

A separable formulation of (1) can be found by recasting it with transformation $G:(\mathbf{x},\mathbf{p})\to(\mathbf{x},\mathbf{v})$, $\mathbf{x}=\mathbf{x}$, $\mathbf{v}=\mathbf{p}/m-q\mathbf{A}(\mathbf{x})/m$, as

$$\begin{aligned}&\dot{\mathbf{x}}=\mathbf{v},\\&\dot{\mathbf{v}}=\frac{q}{m}\big(\mathbf{E}(\mathbf{x})+\mathbf{v}\times\mathbf{B}(\mathbf{x})\big),\end{aligned}\tag{3}$$

where the energy of the system is $H(\mathbf{x},\mathbf{v})=m\mathbf{v}\cdot\mathbf{v}/2+q\varphi(\mathbf{x})$. Denote $\mathbf{z}=[\mathbf{x}^\top,\mathbf{v}^\top]^\top$. Eq. (3) can be written as

$$K(\mathbf{z})\dot{\mathbf{z}}=\nabla H(\mathbf{z}),$$

where $K(\mathbf{z})=\begin{bmatrix}-q\hat{\mathbf{B}}(\mathbf{x}) & -mI\\ mI & 0\end{bmatrix}$ is a skew-symmetric matrix with $\hat{\mathbf{B}}(\mathbf{x})=\begin{bmatrix}0 & -B_3(\mathbf{x}) & B_2(\mathbf{x})\\ B_3(\mathbf{x}) & 0 & -B_1(\mathbf{x})\\ -B_2(\mathbf{x}) & B_1(\mathbf{x}) & 0\end{bmatrix}$ defined by $\mathbf{B}(\mathbf{x})=[B_1(\mathbf{x}),B_2(\mathbf{x}),B_3(\mathbf{x})]^\top$. The skew-symmetric matrix $K(\mathbf{z})$ provides a non-canonical symplectic structure. However, it is a quite difficult task to construct the numerical methods that can preserve the non-canonical structure $K(\mathbf{z})$, while being explicit and cheaper than known symplectic methods.

Let $F(\mathbf{x},\mathbf{v})=[\mathbf{v}^\top,q(\mathbf{E}(\mathbf{x})+\mathbf{v}\times\mathbf{B}(\mathbf{x}))^\top/m]^\top$, it is known that

$$\nabla_{\mathbf{z}}\cdot F=\nabla_{\mathbf{x}}\cdot\mathbf{v}+\frac{q}{m}\nabla_{\mathbf{v}}\cdot\big(\mathbf{E}(\mathbf{x})+\mathbf{v}\times\mathbf{B}(\mathbf{x})\big)\equiv 0,\tag{4}$$

which implies that the vector F is source-free.[1] Denote $\phi_t:\mathbf{z}_0\to\mathbf{z}(t)$ to be the solution flow of system (3). For a region $D(0)$ in phase space $(\mathbf{x},\mathbf{v})$, denote its volume by $V(0)$. Following the solution flow of the system, at time t the region becomes $D(t)=\phi_t D(0)$ whose volume is denoted by $V(t)$. Then,

$$\frac{dV(t)}{dt}=\int_{D(t)}\nabla_{\mathbf{z}}\cdot F d\mathbf{z}\equiv 0.$$

This is Liouville's theorem. So the volume is invariable along the solution flow of system (3), i.e. $V(t)=V(0)$, and $\det(\frac{\partial\phi_t(\mathbf{z}_0)}{\partial\mathbf{z}_0})\equiv 1$.

Besides the volume-preserving property, we observe that along the solution trajectory the energy H is constant for system (3). If the electromagnetic field admits a symmetry with respect to the s-direction, then $p_s=\frac{\partial L}{\partial\dot{x}_s}$ is also a constant according to Noether's theorem. Here, L is the Lagrangian of the system.

At the beginning of this section, we assumed that $\mathbf{B}$ and $\mathbf{E}$ are static. In fact, if $\mathbf{B}$ and $\mathbf{E}$ are both time-dependent, the Lorenz force system in $(\mathbf{x},\mathbf{v})$ has the form

$$K(\mathbf{z},t)\begin{bmatrix}\dot{\mathbf{x}}\\ \dot{\mathbf{v}}\end{bmatrix}=\nabla H+\begin{bmatrix}q\frac{\partial\mathbf{A}}{\partial t}\\ 0\end{bmatrix},\tag{5}$$

where $K(\mathbf{z},t)=\begin{bmatrix}-q\hat{\mathbf{B}}(\mathbf{x},t) & -mI\\ mI & 0\end{bmatrix}$, and $H(\mathbf{z},t)=m\mathbf{v}\cdot\mathbf{v}/2+q\varphi(\mathbf{x},t)$ is the energy. System (5) with time-dependent structure $K(\mathbf{z},t)$ is called the Birkhoffian system which is a generalization of the Hamiltonian system (see Refs. [24] and [25] for more details). It is not an easy task to construct the numerical methods that can preserve the time-dependent structure $K(\mathbf{z},t)$ [26]. As it is investigated that in this case the volume in phase space is also invariant along the solution of the system. The splitting technique developed in the next section can be generalized to this case for presenting the volume-preserving methods.

3. Volume-preserving integrators

It is shown in Section 2 that the system (3) is separable and has the volume-preserving property. In this section, based on the splitting technique we present a class of explicit numerical discretizations which can preserve the volume in the $(\mathbf{x},\mathbf{v})$ coordinates. Systematic development of splitting methods for general systems can be found in Refs. [6,18].

There are different approaches (see [21,23]) for decomposing the system (3). In this paper we mainly focus on the following splitting where the vector field $F(\mathbf{x},\mathbf{v})$ is split into three components:

$$F(\mathbf{x},\mathbf{v})=\begin{bmatrix}\mathbf{v}\\ 0\end{bmatrix}+\begin{bmatrix}0\\ q\mathbf{E}(\mathbf{x})/m\end{bmatrix}+\begin{bmatrix}0\\ q\mathbf{v}\times\mathbf{B}(\mathbf{x})/m\end{bmatrix}:=F_1(\mathbf{x},\mathbf{v})+F_2(\mathbf{x},\mathbf{v})+F_3(\mathbf{x},\mathbf{v}).\tag{6}$$

We observe that each subsystem is a six-dimensional source-free system that can be solved exactly. With a given initial condition $(\mathbf{x}_0,\mathbf{v}_0)$, the solutions of the first and second systems are expressed by the translational transformations

$$\phi_t^{F_1}:\ \begin{cases}\mathbf{x}(t)=\mathbf{x}_0+t\mathbf{v}_0,\\ \mathbf{v}(t)=\mathbf{v}_0,\end{cases}\qquad \phi_t^{F_2}:\ \begin{cases}\mathbf{x}(t)=\mathbf{x}_0,\\ \mathbf{v}(t)=\mathbf{v}_0+tq\mathbf{E}(\mathbf{x}_0)/m.\end{cases}$$

[1] An n-dimensional nonlinear vector f is called source-free if the divergence of $f(x)$ vanishes, that is $\nabla\cdot f:=\sum_{i=1}^n\frac{\partial f_i}{\partial x_i}=0$.

The solution flow $\phi_t^{F_1}$ describes the displacement of the particle position, and $\phi_t^{F_2}$ describes the acceleration of the particle velocity caused by the electric field. We denote by $\mathbf{b}(\mathbf{x})$ the unit vector in the direction of the magnetic field, and $B(\mathbf{x})$ the magnitude of $\mathbf{B}$. The solution of the third subsystem can be expressed explicitly as

$$\phi_t^{F_3}: \quad \begin{cases} \mathbf{x}(t) = \mathbf{x}_0, \\ \mathbf{v}(t) = \exp(t\omega_0\hat{\mathbf{b}}_0)\mathbf{v}_0, \end{cases} \tag{7}$$

with $\omega_0 := -qB(\mathbf{x}_0)/m$ and $\hat{\mathbf{b}}_0 := \hat{\mathbf{b}}(\mathbf{x}_0)$. Here, $\hat{\mathbf{b}}(\mathbf{x})$ is the skew-symmetric matrix

$$\hat{\mathbf{b}}(\mathbf{x}) = \begin{bmatrix} 0 & -b_3(\mathbf{x}) & b_2(\mathbf{x}) \\ b_3(\mathbf{x}) & 0 & -b_1(\mathbf{x}) \\ -b_2(\mathbf{x}) & b_1(\mathbf{x}) & 0 \end{bmatrix}$$

defined by $\mathbf{b}(\mathbf{x}) = [b_1(\mathbf{x}), b_2(\mathbf{x}), b_3(\mathbf{x})]^\top$.

Due to the fact that $\|\mathbf{b}\| = 1$, $\hat{\mathbf{b}}^3 = -\hat{\mathbf{b}}$, the exponential of the matrix $\hat{\mathbf{b}}$ is then a convergent polynomial [6], i.e.

$$\exp(\omega\hat{\mathbf{b}}) = I + \omega\hat{\mathbf{b}} + \frac{1}{2!}\omega^2\hat{\mathbf{b}}^2 + \cdots = I + \sin(\omega)\hat{\mathbf{b}} + \frac{1}{2}\left(\frac{\sin(\omega/2)}{1/2}\right)^2\hat{\mathbf{b}}^2.$$

This, therefore, provides a closed expression of the solution $\mathbf{v}(t)$ in (7),

$$\phi_t^{F_3}(\mathbf{v}_0) = \exp(t\omega_0\hat{\mathbf{b}}_0)\mathbf{v}_0 = \mathbf{v}_0 + \sin(t\omega_0)\hat{\mathbf{b}}_0\mathbf{v}_0 + \big(1 - \cos(t\omega_0)\big)\hat{\mathbf{b}}_0^2\mathbf{v}_0. \tag{8}$$

With $\mathbf{v} = \mathbf{v}_\parallel + \mathbf{v}_\perp$, where $\mathbf{v}_\parallel$ and $\mathbf{v}_\perp$ are the components of $\mathbf{v}$ parallel and perpendicular to $\mathbf{B}$ respectively, (8) can be rewritten as [21]

$$\mathbf{v}(t) = \exp(t\omega_0\hat{\mathbf{b}}_0)\mathbf{v_0} = \mathbf{v}_{0\parallel} + \exp(t\omega_0\hat{\mathbf{b}}_0)\mathbf{v}_{0\perp} = \mathbf{v}_{0\parallel} + \cos(t\omega_0)\mathbf{v}_{0\perp} + \sin(t\omega_0)(\mathbf{b}_0 \times \mathbf{v}_{0\perp}). \tag{9}$$

It means that $\phi_t^{F_3}$ describes the rotation of $\mathbf{v}_\perp$ by $\mathbf{B}$.

In order to construct the numerical methods for system (3), we can compute the third subsystem numerically. Here, we apply the implicit midpoint rule. This gives an approximate solution,

$$\mathbf{v}_1 = \Phi_h^{F_3}(\mathbf{v}_0) = \left(I - \frac{h}{2}\omega_0\hat{\mathbf{b}}_0\right)^{-1}\left(I + \frac{h}{2}\omega_0\hat{\mathbf{b}}_0\right)\mathbf{v}_0 := \mathrm{cay}(h\omega_0\hat{\mathbf{b}}_0)\mathbf{v}_0, \tag{10}$$

where cay is the Cayley transformation [6]. By simple calculation, we have

$$\begin{aligned} \mathbf{v}_1 = \Phi_h^{F_3}(\mathbf{v}_0) &= \mathbf{v}_0 + \frac{4h\omega_0}{4 + h^2\omega_0^2}\mathbf{b}_0 \times \mathbf{v}_0 + \frac{2h^2\omega_0^2}{4 + h^2\omega_0^2}\mathbf{b}_0 \times (\mathbf{b}_0 \times \mathbf{v}_0) \\ &= \mathbf{v_0}_\parallel + \cos(h\tilde{\omega}_0)\mathbf{v_0}_\perp + \sin(h\tilde{\omega}_0)\mathbf{b_0} \times \mathbf{v_0}_\perp, \end{aligned} \tag{11}$$

where $\tilde{\omega}_0$ is an approximate local cyclotron frequency connected to ω_0 by

$$h\omega_0/2 = \tan(h\tilde{\omega}_0/2).$$

The map $\Phi_h^{F_3}$ is time-symmetric, i.e., $\Phi_h^{F_3} = (\Phi_{-h}^{F_3})^{-1}$. By Taylor's expansion, it shows that the map $\Phi_h^{F_3}$ is a second order approximation to the exact solution flow $\phi_h^{F_3}$ (8).

Though we can use other numerical methods to solve the subsystem $\dot{\mathbf{z}} = F_3(\mathbf{z})$, it should be noticed that only the exact flows $\phi_h^{F_3}$ (8) and $\Phi_h^{F_3}$ (10) are volume-preserving. This can be explained by analyzing the linear systems. Consider an n-dimensional linear source-free system $\dot{x} = Ax$ with $A \in sl(n) := \{A \in \mathbb{R}^{n\times n};\ \mathrm{trace}(A) = 0\}$. The numerical solution $x_{k+1} = \psi(hA)x_k$ is volume-preserving iff $\det(\psi(hA)) = 1$, that is

$$\psi(hA) \in SL(n) := \big\{Q \in \mathbb{R}^{n\times n};\ \det(Q) = 1\big\}.$$

It has been proved in [17] that there is no other consistent analytic map than the exponential exp itself that can map $sl(n)$ to $SL(n)$. This leads to that conventional methods, generally, are not volume-preserving [17]. However, in the case of $n = 3$, the implicit midpoint rule which is induced by the Cayley transformation, is an exception. In fact, let the Cayley transformation be

$$\mathrm{cay}(hA) = (I - hA/2)^{-1}(I + hA/2),$$

where $A \in sl(3)$. It can be proved that $\det(\mathrm{cay}(hA)) = 1$ if and only if $\det(A) = 0$ (see p. 141 of [6] or [17]). From (10), and the fact that $\hat{\mathbf{b}} \in sl(3)$ and $\det(\hat{\mathbf{b}}) = 0$, it is known that $\det(\mathrm{cay}(h\omega\hat{\mathbf{b}})) = 1$. This implies that the map $\Phi_h^{F_3}$ in (10) induced by the Cayley transformation is volume-preserving.

Volume-preserving numerical methods of any order can be constructed by various composition of $\varphi_h^{F_1}$, $\varphi_h^{F_2}$, $\varphi_h^{F_3}$ or $\Phi_h^{F_3}$ [6,17,18]. For the Lorentz force system, by applying Lemma 3 in [17] we obtain the following proposition which gives a simple and efficient way to construct volume-preserving numerical methods of high order.

Proposition 3.1. *Assume that the Lorentz force system (3) is decomposed as three subsystems with vector fields F_i, $i = 1, 2, 3$. Let $\phi_t^{F_i}$ be the flow of the i-th subsystem, then we can construct the volume-preserving numerical method*

- *of order* 1 *as*

$$G_h^1 := \phi_h^{F_1} \circ \phi_h^{F_2} \circ \phi_h^{F_3} \quad or \quad G_h^{1*} := \left(G_{-h}^1\right)^{-1} = \phi_h^{F_3} \circ \phi_h^{F_2} \circ \phi_h^{F_1};$$

- *of order* 2 *and symmetric as*

$$G_h^2 := G_{h/2}^1 \circ G_{h/2}^{1*} = \phi_{h/2}^{F_1} \circ \phi_{h/2}^{F_2} \circ \phi_h^{F_3} \circ \phi_{h/2}^{F_2} \circ \phi_{h/2}^{F_1};$$

- *of order* $2(l+1)$ *and symmetric as*

$$G_h^{2(l+1)} := G_{\alpha_l h}^{2l} \circ G_{\beta_l h}^{2l} \circ G_{\alpha_l h}^{2l},$$

where h is the time step, $\alpha_l = (2 - 2^{1/(2l+1)})^{-1}$ and $\beta_l = 1 - 2\alpha_l < 0$.

Replacing the exact flow $\phi_h^{F_i}$, $i = 1, 2, 3$, by a p-th order approximation method $\Phi_h^{F_i}$, if $\Phi_h^{F_i}$ is symmetric and volume-preserving, then the above results still hold.

Applying Proposition 3.1, we present the following volume-preserving methods that can be computed explicitly. We denote the time-step by h and the numerical solution at kh by $(\mathbf{x}_k, \mathbf{v}_k)$. For simplicity, we use the notations $\omega_k := -qB(\mathbf{x}_k)/m$, $\mathbf{b}_k := \mathbf{B}(\mathbf{x}_k)/B(\mathbf{x}_k)$ and $\mathbf{E}_k := \mathbf{E}(\mathbf{x}_k)$.

First order methods. The first-order volume-preserving method for system (3) constructed by the composition $G_h^1 := \phi_h^{F_1} \circ \phi_h^{F_2} \circ \phi_h^{F_3}$ reads

$$\begin{aligned}
&\mathbf{v}^- = \exp(h\omega_k \hat{\mathbf{b}}_k)\mathbf{v}_k,\\
&\mathbf{v}_{k+1} = \mathbf{v}^- + \frac{hq}{m}\mathbf{E}_k,\\
&\mathbf{x}_{k+1} = \mathbf{x}_k + h\mathbf{v}_{k+1},
\end{aligned} \tag{12}$$

where $\mathbf{x}_k \approx \mathbf{x}(t_k)$, $\mathbf{v}_k \approx \mathbf{v}(t_k)$, and $\exp(h\omega_k \hat{\mathbf{b}}_k)$ is calculated by formula (8). Replacing $\phi_h^{F_3}$ by $\Phi_h^{F_3}$, we can get an alternative method of first order,

$$\begin{aligned}
&\mathbf{v}^- = \mathbf{v}_k + \frac{h\omega_k}{2}\mathbf{b}_k \times \left(\mathbf{v}_k + \mathbf{v}^-\right),\\
&\mathbf{v}_{k+1} = \mathbf{v}^- + \frac{hq}{m}\mathbf{E}_k,\\
&\mathbf{x}_{k+1} = \mathbf{x}_k + h\mathbf{v}_{k+1}.
\end{aligned} \tag{13}$$

Eliminating $\mathbf{v}^-$ and using (8) and (11), schemes (12) and (13) can be reduced to

$$\begin{cases}
\mathbf{v}_{k+1} = \mathbf{v}_k + \alpha\mathbf{b}_k \times \mathbf{v}_k + \beta\mathbf{b}_k \times (\mathbf{b}_k \times \mathbf{v}_k) + \dfrac{hq}{m}\mathbf{E}_k,\\
\mathbf{x}_{k+1} = \mathbf{x}_k + h\mathbf{v}_{k+1},
\end{cases}$$

with $\alpha = \sin(h\omega_k)$, $\beta = (1 - \cos(h\omega_k))$ for (12), and $\alpha = \frac{4h\omega_k}{4+(h\omega_k)^2}$, $\beta = \frac{2(h\omega_k)^2}{4+(h\omega_k)^2}$ for (13).

Second order symmetric method. The second order symmetric method for system (3) constructed by a composition $G_h^2 := \phi_{\frac{h}{2}}^{F_1} \circ \phi_{\frac{h}{2}}^{F_2} \circ \phi_h^{F_3} \circ \phi_{\frac{h}{2}}^{F_2} \circ \phi_{\frac{h}{2}}^{F_1}$ is

$$\begin{aligned}
&\mathbf{x}_{k+\frac{1}{2}} = \mathbf{x}_k + \frac{h}{2}\mathbf{v}_k,\\
&\mathbf{v}^- = \mathbf{v}_k + \frac{hq}{2m}\mathbf{E}_{k+\frac{1}{2}},\\
&\mathbf{v}^+ = \exp(h\omega_{k+\frac{1}{2}}\hat{\mathbf{b}}_{k+\frac{1}{2}})\mathbf{v}^-,\\
&\mathbf{v}_{k+1} = \mathbf{v}^+ + \frac{hq}{2m}\mathbf{E}_{k+\frac{1}{2}},\\
&\mathbf{x}_{k+1} = \mathbf{x}_{k+\frac{1}{2}} + \frac{h}{2}\mathbf{v}_{k+1}.
\end{aligned} \tag{14}$$

Noticing that the computation of $\mathbf{v}_{k+1}$ only needs the value of $\mathbf{x}$ at $(k+\frac{1}{2})h$, then we can apply a staggered time grid. Let $\mathbf{x}_k \approx \mathbf{x}(kh)$ and $\mathbf{v}_k \approx \mathbf{v}(kh-\frac{h}{2})$. Scheme (14) is identical to

$$G_h^2: \quad \begin{cases} \mathbf{v}_{k+1} = \exp(h\omega_k \hat{\mathbf{b}}_k)\left(\mathbf{v}_k + \dfrac{hq}{2m}\mathbf{E}_k\right) + \dfrac{hq}{2m}\mathbf{E}_k, \\ \mathbf{x}_{k+1} = \mathbf{x}_k + h\mathbf{v}_{k+1}. \end{cases} \tag{15}$$

Replacing $\phi_h^{F_3}$ by $\Phi_h^{F_3}$ in G_h^2, this provides an alternative second order method on a staggered grid

$$\widetilde{G}_h^2: \quad \begin{cases} \mathbf{x}_{k+1} = \mathbf{x}_k + h\mathbf{v}_{k+1}, \\ \mathbf{v}_{k+1} = \mathbf{v}_k + \dfrac{hq}{m}\mathbf{E}_k + \dfrac{h}{2}\omega_k \mathbf{b}_k \times (\mathbf{v}_{k+1} + \mathbf{v}_k). \end{cases} \tag{16}$$

Scheme (16) is, in fact, the Boris algorithm. It has been proved in [13] that the Boris algorithm is volume-preserving. Our analysis shows that the Boris algorithm can be interpreted as a composition of volume-preserving maps, which provides another way to verify its volume-preserving property.

High order symmetric method. The symmetric volume-preserving numerical methods of arbitrary high order can be constructed by taking (12)–(16) as the basis. For example, the numerical methods of fourth order can be constructed as

$$G_h^4 = G_{\gamma_1 h}^2 \circ G_{\gamma_0 h}^2 \circ G_{\gamma_1 h}^2, \qquad \widetilde{G}_h^4 = \widetilde{G}_{\gamma_1 h}^2 \circ \widetilde{G}_{\gamma_0 h}^2 \circ \widetilde{G}_{\gamma_1 h}^2, \tag{17}$$

where $\gamma_1 = (2-2^{1/3})^{-1}$ and $\gamma_0 = 1-2\gamma_1$.

The above volume-preserving methods designed using the splitting technique are all explicit and easy to compute. To discuss their stability, we take the test equation to be

$$\dot{\mathbf{x}} = \mathbf{v}, \qquad \dot{\mathbf{v}} = \Lambda \mathbf{x} + \mathbf{B} \times \mathbf{v},$$

where $\Lambda = \mathrm{diag}(-\lambda^2, -\lambda^2, \lambda_z)$ is the diagonalization of the Jacobian matrix $\nabla^2\varphi(\mathbf{x}_0)$, $\mathbf{B} = \omega \mathbf{e}_z$ is a constant vector. Denote the time step by h. The second order methods (15) and (16) are linearly stable if

$$|h\lambda| \le 2 \quad \left(\text{and } h\omega \ne k\pi,\ \forall k \in \mathbb{Z} \text{ for } G_h^2\right).$$

For the Boris method, this is a well known result [10]. The above second and fourth order methods can be unconditionally stable (except the unstable points $h\omega = k\pi$ for G_h^2 and G_h^4) if the electric field is absent. Although these numerical methods are stable in almost the entire phase space, to simulate accurately the Larmor cyclotron we need to choose the time step satisfying $h\omega \le \pi$ according to the Nyquist limit. Furthermore, methods derived with the exact flow $\phi_h^{F_3}$ are more accurate than that with the approximate flow $\Phi_h^{F_3}$. Thus, to achieve a numerical solution with a given accuracy the time step restriction can be loosened.

4. Numerical experiments

In this section, we numerically test the volume-preserving methods constructed in Section 3.

4.1. 2D dynamics in a static electromagnetic field

Firstly, we consider the 2D dynamics of the charged particle in a static, non-uniform electromagnetic field

$$\mathbf{B} = \nabla \times \mathbf{A} = R\mathbf{e}_z, \qquad \mathbf{E} = -\nabla\varphi = \frac{10^{-2}}{R^3}(x\mathbf{e}_x + y\mathbf{e}_y), \tag{18}$$

where the potentials are chosen to be $\mathbf{A} = R^2/3\mathbf{e}_\xi$, $\varphi = \frac{10^{-2}}{R}$ in cylindrical coordinates (R, ξ, z) with $R = \sqrt{x^2+y^2}$. In this example, the physical quantities are normalized by the system size a, the characteristic magnetic field B_0, and the gyro-frequency $\omega_0 \equiv qB_0/m$ of the particle. The Lagrangian is $L = (\dot{R}^2 + R^2\dot{\xi}^2 + \dot{z}^2)/2 + R\dot{\xi}A_\xi - \varphi$. Due to $\partial L/\partial\xi \equiv 0$, the angular momentum

$$p_\xi = R^2\dot{\xi} + R^3/3$$

is invariant along the solution trajectory of system (3). It is known that the energy

$$H = \frac{1}{2}\mathbf{v}\cdot\mathbf{v} + \frac{10^{-2}}{R}$$

is a constant of motion. As the given electromagnetic field (18) changes slowly with respect to the spatial period of the motion, the magnetic moment $\mu = v_\perp^2/(2R)$ is an adiabatic invariant.

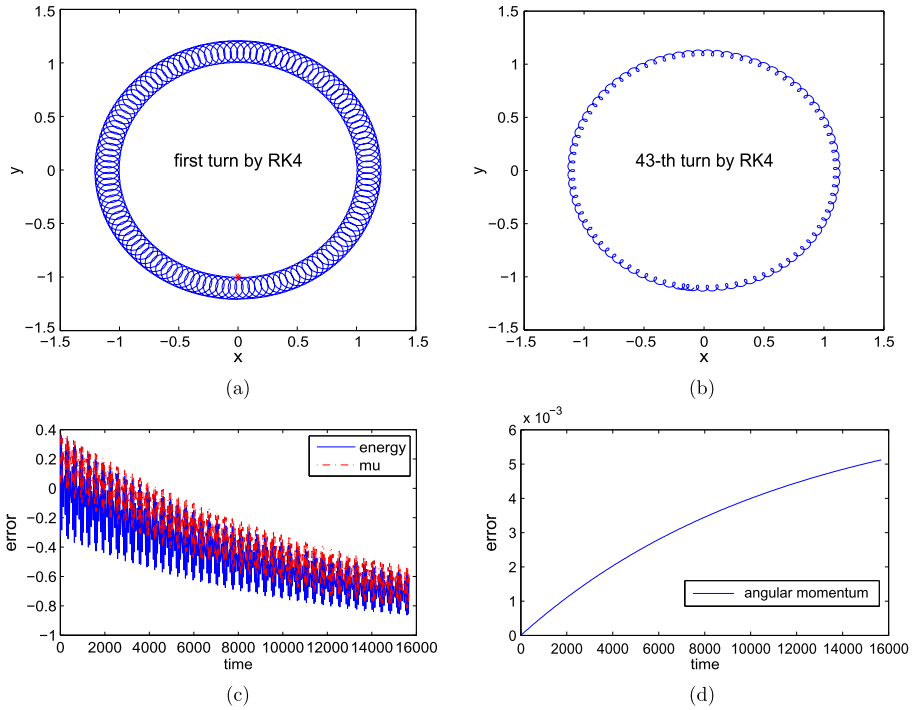

Fig. 1. The fourth order explicit method *RK*4 is applied to the simple 2D dynamics with step size $h = \pi/10$. (a): The orbit in the first 2300 steps. (b): The orbit after 10^5 steps. The bottom two figures show the normalized errors of invariants as a function of time $t = Nh$. (c): Energy H (blue solid line) and magnetic moment μ (red dashed line). (d): Angular momentum p_ξ.

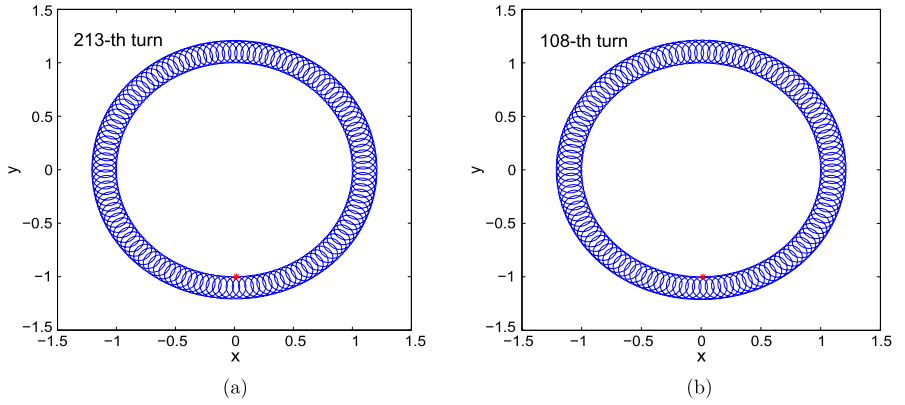

Fig. 2. Numerical orbits of the volume-preserving methods with time step $h = \pi/10$. (a): The orbit after 5×10^5 steps by the second order methods. (b): The orbit after 2.5×10^5 steps by the fourth order methods.

Starting from the initial position $\mathbf{x}_0 = [0, -1, 0]^\top$ with the initial velocity $\mathbf{v}_0 = [0.1, 0.01, 0]^\top$, the analytic orbit of the charged particle is a spiraling circle with constant radius. The large circle corresponds to the $\nabla \cdot \mathbf{B}$ drift and the $\mathbf{E} \times \mathbf{B}$ drift of the guiding center, and the small circle is the fast-scale gyro-motion.

We first apply the Runge–Kutta method of order four denoted by *RK*4 and the numerical results are shown in Fig. 1. The step size is $h = \pi/10$ which is the 1/20 of the characteristic gyro-period. Though *RK*4 has a fourth order of accuracy, the numerical error accumulation after 10^5 steps gives rise to a complete wrong solution orbit in Fig. 1(b), where the gyro-motion is numerically dissipated. The normalized errors of the invariants as a function of integration time are performed in Fig. 1(c) and (d). These figures show that the *RK*4 cannot preserve the invariants inherited by this system. This explains the numerical behaviors of the orbits plotted in Fig. 1(a) and (b).

Next, we test the volume-preserving numerical methods. Fig. 2 shows the numerical orbits of the second order methods after 5×10^5 steps in (a), and that of the fourth order methods after 2.5×10^5 steps in (b). The volume-preserving methods provide a correct and stable gyro-motion over a very long integration time.

In Fig. 3, we illustrate the relative errors of the energy H, the angular momentum p_ξ and the magnetic moment μ computed by the four volume-preserving numerical methods G_h^2, $\widetilde{G}_h^2$, G_h^4 and $\widetilde{G}_h^4$ over 5×10^4 steps. It is observed that the

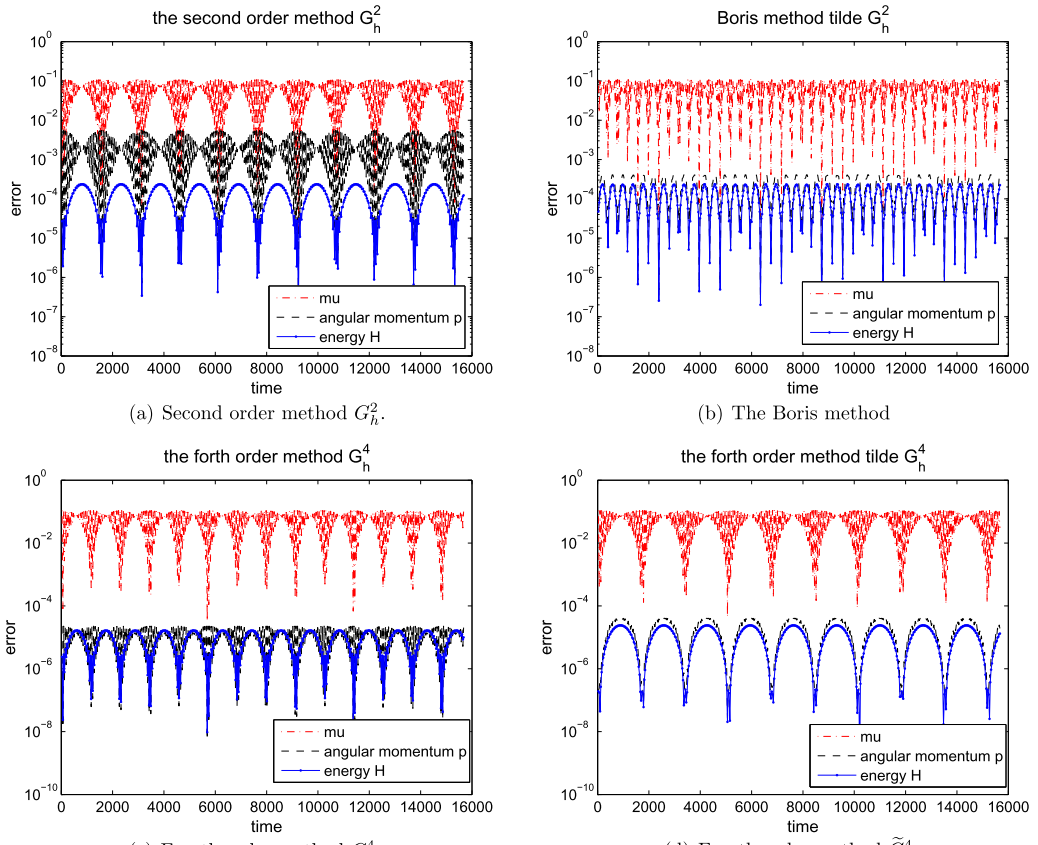

(a) Second order method G_h^2. (b) The Boris method

(c) Fourth order method G_h^4 (d) Fourth order method $\widetilde{G}_h^4$

Fig. 3. Relative errors of the energy H, the angular momentum p_ξ and the magnetic moment μ as a function of time $t \equiv nh$. The step size is $h = \pi/10$, and the integration time interval is $[0, 5 \times 10^4 h]$.

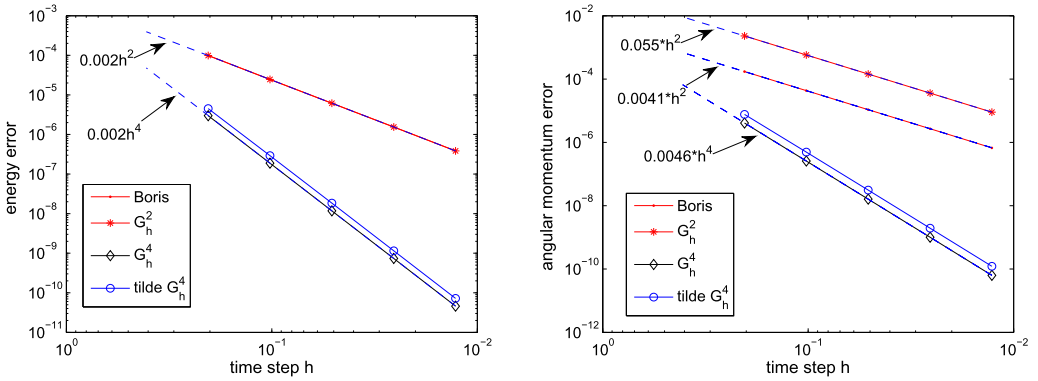

Fig. 4. Numerical errors of invariants in the infinity norm as a function of step size h. The relative errors are computed till $t = 39.17$. Left: The errors of the energy. Right: The errors of the angular momentum.

errors are bounded over a long integration time. Except the adiabatic invariant μ, the errors of other invariants become smaller when the higher order methods are used. To analyze further, in Fig. 4 we plot the errors of the invariants H and p_ξ in infinity norm as functions of the step size h. We observe that the invariant errors are about a scale of h^2 for G_h^2 and the Boris method, and a scale of h^4 for the fourth order methods G_h^4 and $\widetilde{G}_h^4$. In Fig. 3(b), it is noticed that the Boris method preserves the angular momentum p_ξ slightly better than G_h^2. However, this is not a general rule. The errors of p_ξ computed by the two methods are both of order two. For this example, it can be seen clearly from Fig. 4 that the error of p_ξ for the Boris method is about $0.0041h^2$, and that for G_h^2 is $0.055h^2$, which implies that the Boris scheme has a smaller truncation coefficient. If the initial values or electromagnetic fields change, the truncation constants of errors of p_ξ for G_h^2 and $\widetilde{G}_h^2$ (the Boris scheme) will change.

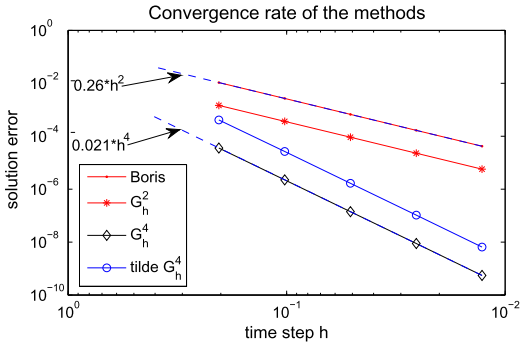

Fig. 5. Convergence rates of numerical solutions by the volume-preserving methods G_h^2, the Boris method, G_h^4 and $\widetilde{G}_h^4$. The errors are computed in the l_2 norm.

In Fig. 5, we compute the convergence rate of the four volume-preserving numerical methods. The global error $\|[\mathbf{x}_n, \mathbf{v}_n] - [\mathbf{x}(nh), \mathbf{v}(nh)]\|_2$ is computed at time $t \equiv nh = 39.17$. It is shown that the method G_h^2 and the Boris method have the convergence rate of order two; the methods G_h^4 and $\widetilde{G}_4^h$ have the convergence rate of order four. It is also noticed that the method G_h^2 (or G_h^4) is more accurate than the Boris method (or $\widetilde{G}_h^4$).

4.2. 2D dynamics in an axisymmetric tokamak geometry

In this subsection, we consider the motion of a charged particle in a 2-dimensional axisymmetric tokamak geometry without inductive electric field.

The magnetic field in the toroidal coordinates (r, θ, ξ) is expressed as

$$\mathbf{B} = \frac{B_0 r}{qR}\mathbf{e}_\theta + \frac{B_0 R_0}{R}\mathbf{e}_\xi, \tag{19}$$

where $B_0 = 1$, $R_0 = 1$, and $q = 2$ are constant with their usual meanings. The corresponding vector potential $\mathbf{A}$ is chosen to be

$$\mathbf{A} = \frac{z}{2R}\mathbf{e}_R + \frac{(1-R)^2 + z^2}{4R}\mathbf{e}_\xi - \frac{\ln R}{2}\mathbf{e}_z.$$

In this example, the physical quantities are normalized by the system size a, characteristic magnetic field B_0, and the gyro-frequency $\omega_0 \equiv qB_0/m$. In the absence of electric field, the Hamiltonian (energy) of the system is $H = \mathbf{v}\cdot\mathbf{v}/2$, which is a constant of motion. As $\mathbf{A}$ is axisymmetric, the angular momentum $p_\xi = \frac{\partial L}{\partial \dot{\xi}}$ is invariant along the solution trajectory of the system. The magnetic moment $\mu = v_\perp^2/\|\mathbf{B}(\mathbf{x})\|$ is still an adiabatic invariant. With the conserved quantities, the solution orbit projected on (R, z) space forms a closed orbit.

To apply the volume-preserving numerical methods constructed in Section 3, we transform $\mathbf{B}$ (19) into the Cartesian coordinates (x, y, z) which is

$$\mathbf{B} = -\frac{2y + xz}{2R^2}\mathbf{e}_x + \frac{2x - yz}{2R^2}\mathbf{e}_y + \frac{1}{2R}(R-1)\mathbf{e}_z.$$

Starting with the initial position $\mathbf{x}_0 = [1.05, 0, 0]^\top$ and the initial velocity $\mathbf{v}_0 = [0, 4.816\text{e}{-4}, -2.059\text{e}{-3}]^\top$, the orbit projected on (R, z) space is a banana orbit, and it will turn into a transit orbit when the initial velocity is changed to $\mathbf{v}_0 = [0, 2\times 4.816\text{e}{-4}, -2.059\text{e}{-3}]^\top$. Setting the step size $h = \pi/10$, which is 1/20 of the gyro-period, we adopt the *RK*4 and the volume-preserving methods developed above. The simulation over 5×10^4 steps is shown in Fig. 6. For the results generated by the *RK*4 in Fig. 6(a) and (b), due to the numerical damping of energy the numerical orbits are not closed, and the gyro-motion is dissipated. The banana orbit gradually transformed into a circulating orbit and the transit orbit deviates to the right side. By comparison, in Fig. 6(c)–(d) the volume-preserving methods give correct and qualitatively better orbits over a very long integration time.

In the case without an electric field, the volume-preserving methods derived in this paper can preserve the energy H exactly. In Fig. 7 we display the relative errors of the energy. It can be observed in Fig. 7(b) that the errors of the energy are up to the round-off error of 10^{-14}, while in Fig. 7(a) the energy computed by the *RK*4 dissipates with time.

The above experiments show the superiority of the newly derived volume-preserving numerical methods over non-geometric numerical methods for solving the Lorenz force system with a static electromagnetic field. In the following, this method is extended to the study of the motion of a charged particle in a time-dependent electromagnetic field.

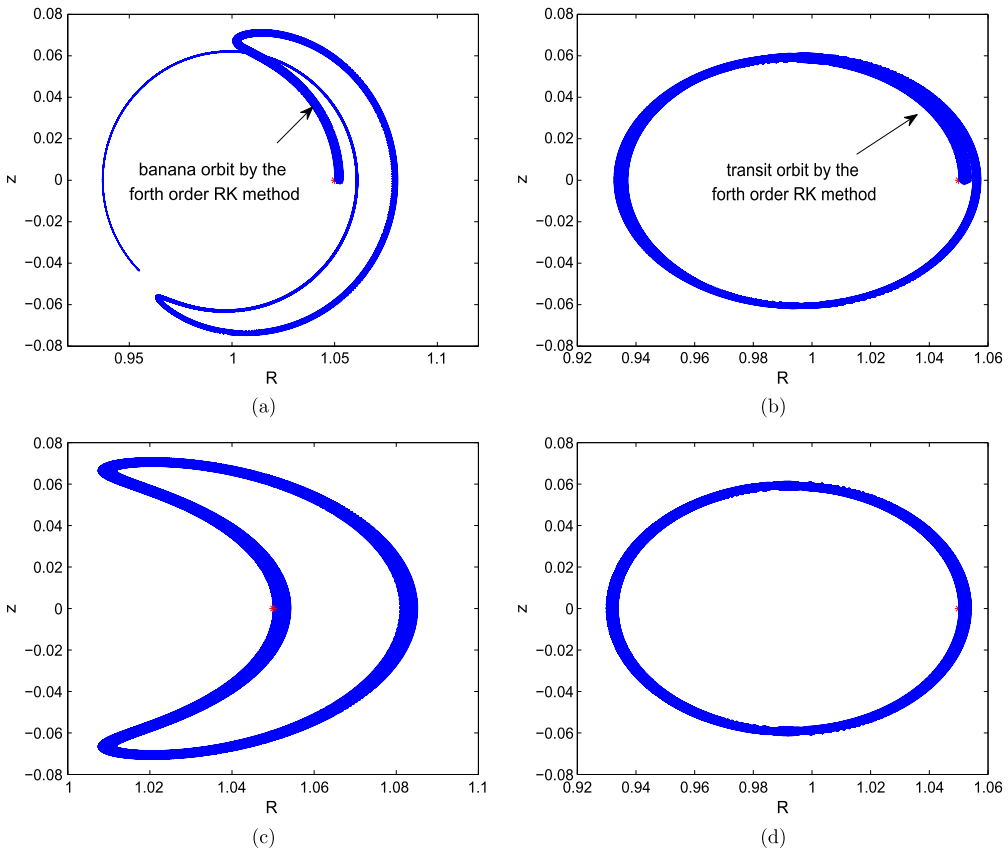

Fig. 6. Numerical orbits. (a): Banana orbit by the *RK*4. (b): Transit orbit by the *RK*4. (c): Banana orbit by the volume-preserving methods. (d): Transit orbit by the volume-preserving methods. The step size is $h = \pi/10$, and the integration interval is $[0, 5 \times 10^5 h]$.

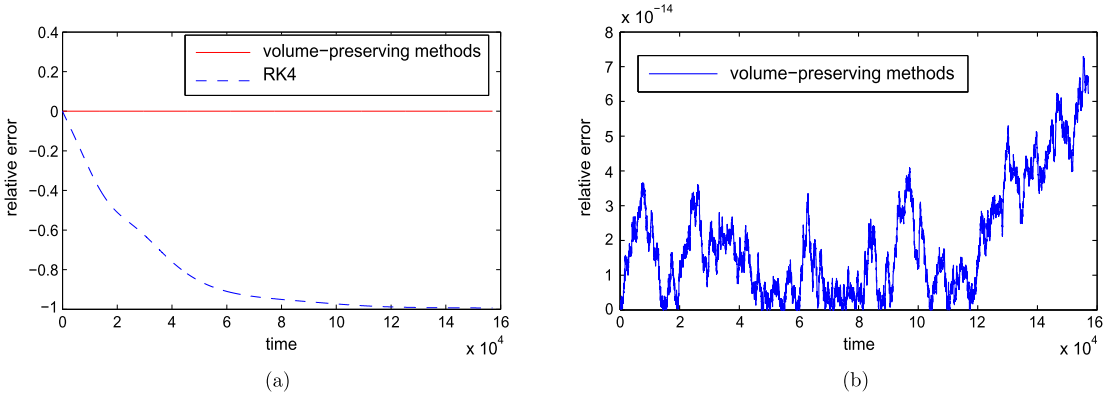

Fig. 7. Relative errors of the energy H as a function of time t. The step size is $h = \pi/10$, and the integration interval is $[0, 5 \times 10^5 h]$. (a): Comparison between the *RK*4 and the volume-preserving methods. (b): Energy preservation of the volume-preserving methods.

4.3. 2D dynamics in a time-dependent electromagnetic field

In this subsection, we solve numerically the system (3) in a time-dependent electromagnetic field. In this case, the system still possesses an invariant phase space volume. The numerical methods based on splitting technique presented in Section 3 can also be applied to give numerical algorithms that can preserve the volume in phase space. For convenience, we assume that the magnetic field $\mathbf{B} = R\mathbf{e}_z$ is static and the electric field is time-dependent which is expressed as

$$\mathbf{E} = -\nabla\varphi = \frac{10^{-2}}{R^3}[x, y, 0]\cos(\gamma t) \quad \text{with } \varphi = \frac{10^{-2}}{R}\cos(\gamma t).$$

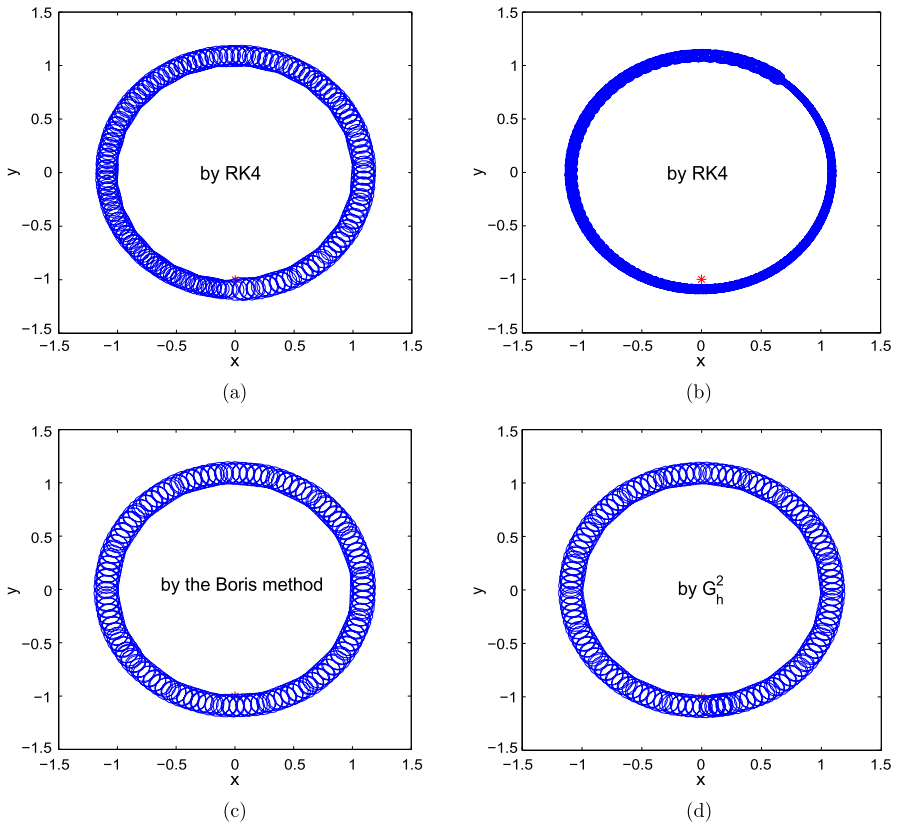

Fig. 8. Orbits in a time-dependent electromagnetic field. Time step is $h = 0.125\pi$. (a): The orbit of the first 4000 steps given by *RK4*. (b): The orbit after 1.4×10^4 steps computed by *RK4*. (c): The orbit after 3.5×10^4 steps given by the Boris method. (d): The orbit after 3.5×10^4 steps computed by G_h^2.

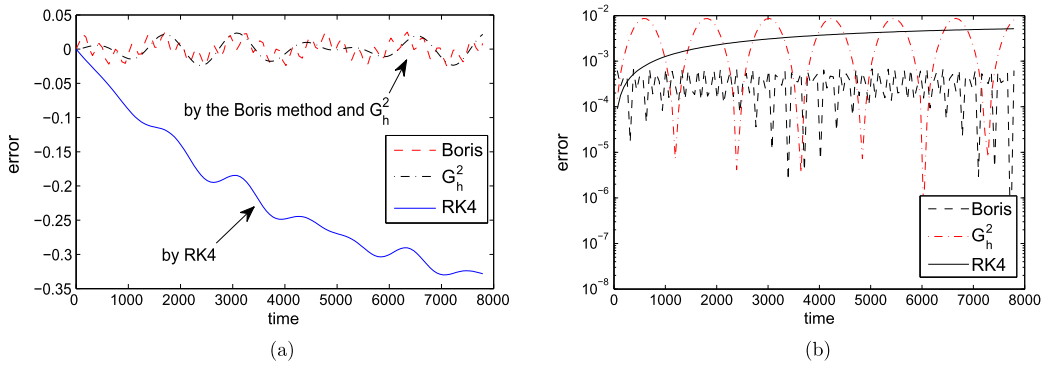

Fig. 9. Normalized errors of the energy and the angular momentum. Time step is $h = 0.125\pi$. (a): Energy error calculated by $(H(\mathbf{x}_n, nh) - H(\mathbf{x}(nh), nh))/|H(\mathbf{x}(nh), nh)|$; (b): Angular momentum error.

The physical quantities are normalized as in the first experiment. As the electric field is varying with time, the energy is no longer a constant of motion. In this example, the angular momentum is still a constant of motion.

The frequency γ is chosen to be $\gamma = 0.5$. Take the initial conditions to be $\mathbf{x}_0 = [0, -1, 0]^\top$ and $\mathbf{v}_0 = [0.1, 0.01, 0]^\top$. The computation is done over the time interval $[0, 4 \times 10^4 h]$ with the time step $h = 0.125\pi$, which is the $1/16$ of the characteristic gyro-period.

In Fig. 8, it is shown that the gyro-motion computed by the *RK4* after a long time of integration dissipates, while the orbits computed by the volume-preserving methods G_h^2 and the Boris method remain closed with a bounded gyro-motion radius.

Fig. 9 shows the normalized errors of the energy (in (a)) and the angular momentum (in (b)) over the time interval $[0, 2 \times 10^4 h]$. The errors of the energy are computed with $(H(\mathbf{x}_n, nh) - H(\mathbf{x}(nh), nh))/|H(\mathbf{x}(nh), nh)|$, where $\mathbf{x}(t)$ is gained by the *RK4* with a very small step size. The main observation is that the numerical quantities oscillate around the exact

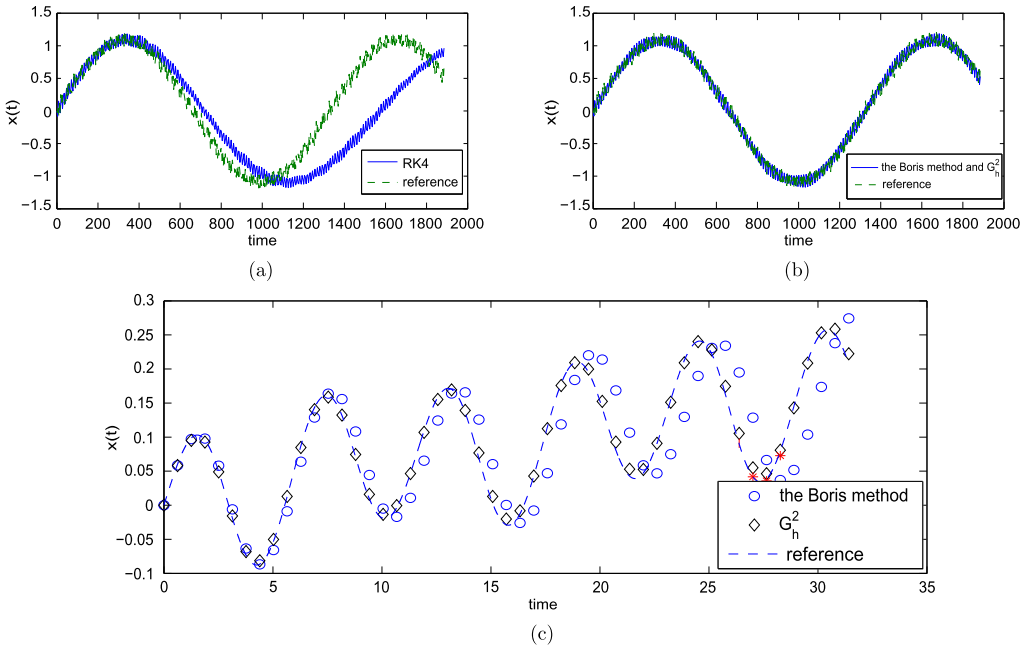

Fig. 10. Numerical solutions in the x-direction. (a): By the $RK4$ with $h = 0.125\pi$. (b): By the Boris method and G_h^2 with $h = 0.125\pi$. (c): By the Boris method and G_h^2 with $h = 0.2\pi$. The reference solution is computed by the fourth order Suzuki composition with small step size. The electromagnetic field is $\mathbf{B} = R\mathbf{e}_z$. $\varphi = 0.01/R\cos(0.5t)$.

ones with no drift for the Boris method and the method G_h^2, but for the $RK4$ the energy is dissipative, and the angular momentum is not preserved.

In Fig. 10, we compare the numerical solutions with the reference solution in the x-direction. The reference solution (dashed line) is given by the fourth order Suzuki composition [27] with a very small time step. In (a) and (b), the numerical solutions are computed with time step $h = 0.125\pi$ during one period of the slow-scale motion. Due to numerical energy dissipation of the $RK4$, it can be seen from (a) that the solution drifts forward after half of the period, i.e. the numerical frequency of the slow-scale periodic motion diminishes after a long time of integration. Meanwhile, in (b) the solution of the volume-preserving methods show a secular consistency with the reference solution. The solutions during the first 5 periods of the gyro-motion are compared in (c). The time step is chosen to be $h = 0.2\pi$ which is the $1/10$ of the characteristic gyro-period. The algorithms developed in the current manuscripts can be applied without modification to the cases where the electromagnetic field is self-consistently determined from the charged particles. Studies in this topic will be reported in future publications.

5. Concluding remarks

It is well-known that the geometric numerical integrators have played an important role in long time simulation for dynamical systems. This paper is devoted to constructing the volume-preserving methods for the Lorenz force system. In the coordinates $(\mathbf{x}, \mathbf{v})$, the Lorenz force system has a non-canonical structure. But usually it is not easy to construct the numerical methods which can preserve the non-canonical structure, while being explicit and cheaper than known symplectic methods. It has been noticed that this system has an invariant volume form in phase space. Under certain symmetries, it has other invariants such as the energy, the angular momentum and the magnetic moment. We have shown that the Lorenz force system can be split as three solvable source-free subsystems. Based on the splitting technique, we have designed a class of explicit volume-preserving methods that can be arbitrarily high order. The Boris method, a popular method in plasma physics, can be fitted in this framework as a composition of volume-preserving maps. This confirms again the volume-preserving nature of the Boris method. Furthermore, the newly developed splitting methods can bound the errors of conserved quantities, and have demonstrated the superior numerical properties of numerical solutions over long simulation time.

For a given static electromagnetic field, we have shown that the volume-preserving methods can bound the errors of the invariants up to the order of the method. The study can be generalized to the cases with time-dependent electromagnetic field. Though in this case, the energy is not constant along the solution trajectory, the errors of the energy computed by the volume-preserving methods are still globally bounded for all simulation time steps. Further analysis about the long term properties of the volume-preserving numerical methods will be done in our future work.

Acknowledgements

This research was supported by the National Natural Science Foundation of China (11271357, 11075162, 11261140328), by CSC, the CAS Program for Interdisciplinary Collaboration Team, the Foundation for Innovative Research Groups of the NNSFC (11321061), the National Basic Research Program of China (2010CB832702) and the ITER–China Program (2014GB124005).

References

[1] P.M. Bellan, Fundamentals of Plasma Physics, 1st edition, Cambridge University Press, 2008.
[2] R.G. Littlejohn, Variational principles of guiding centre motion, J. Plasma Phys. 29 (1983) 111–125.
[3] H. Qin, X. Guan, Variational symplectic integrator for long-time simulations of the guiding-center motion of charged particles in general magnetic fields, Phys. Rev. Lett. 100 (2008) 035006.
[4] H. Qin, X. Guan, W.M. Tang, Variational symplectic algorithm for guiding center dynamics and its application in tokamak geometry, Phys. Plasmas 16 (2009) 042510.
[5] Z. Shang, KAM theorem of symplectic algorithms for Hamiltonian systems, Numer. Math. 83 (3) (1999) 477–496.
[6] E. Hairer, C. Lubich, G. Wanner, Geometric Numerical Integration: Structure-Preserving Algorithms for Ordinary Differential Equations, 2nd edition, Springer-Verlag, Berlin, 2006.
[7] R.G. Littlejohn, Hamiltonian formulation of guiding center motion, Phys. Fluids 24 (9) (1981) 1730–1749.
[8] P.J. Morrison, J.M. Greene, Noncanonical Hamiltonian density formulation of hydrodynamics and ideal magnetohydrodynamics, Phys. Rev. Lett. 45 (1980) 790–794.
[9] E. Hairer, S.P. Nørsett, G. Wanner, Solving Ordinary Differential Equations. I—Nonstiff Problems, 2nd edition, Springer Ser. Comput. Math., vol. 8, Springer-Verlag, Berlin, 1993.
[10] C.K. Birdsall, A.B. Langdon, Plasma Physics via Computer Simulation, Ser. Plasma Phys., Taylor & Francis, 2005.
[11] J. Boris, in: Proceedings of the Fourth Conference on Numerical Simulation of Plasmas, Naval Research Laboratory, Washington D.C., 1970, pp. 3–67.
[12] P.H. Stoltz, J.R. Cary, G. Penn, J. Wurtele, Efficiency of a Boris like integration scheme with spatial stepping, Phys. Rev. Spec. Top., Accel. Beams 5 (2002) 094001.
[13] H. Qin, S. Zhang, J. Xiao, J. Liu, Y. Sun, W.M. Tang, Why is Boris algorithm so good?, Phys. Plasmas 20 (2013) 084503.
[14] Z. Shang, Construction of volume-preserving difference schemes for source-free systems via generating functions, J. Comput. Math. 12 (3) (1994) 265–272.
[15] Y. Sun, A class of volume-preserving numerical algorithms, Appl. Math. Comput. 206 (2) (2008) 841–852.
[16] K. Feng, Symplectic, contact and volume-preserving algorithms, in: Z.C. Shi, T. Ushijima (Eds.), Proc. 1st China–Japan Conf. on Computation of Differential Equations and Dynamical Systems, World Scientific, Singapore, 1993, pp. 1–28.
[17] K. Feng, Z. Shang, Volume-preserving algorithms for source-free dynamical systems, Numer. Math. 71 (1995) 451–463.
[18] R.I. McLachlan, G.R.W. Quispel, Splitting methods, Acta Numer. 11 (2002) 341–434.
[19] J.M. Finn, L. Chacón, Volume preserving integrators for solenoidal fields on a grid, Phys. Plasmas 12 (2005) 054503.
[20] N. Crouseilles, M. Mehrenberger, E. Sonnendrücker, Conservative semi-Lagrangian schemes for the Vlasov equation, J. Comput. Phys. 229 (2010) 1927–1953.
[21] S.A. Chin, Symplectic and energy-conserving algorithms for solving magnetic field trajectories, Phy. Rev. E 77 (2008) 066401.
[22] Y.K. Wu, E. Forest, D.S. Robin, Explicit symplectic integrator for s-dependent static magnetic field, Phys. Rev. E 68 (2003) 046502.
[23] L. Patacchini, I.H. Hutchinson, Explicit time-reversible orbit integration in Particle In Cell codes with static homogeneous magnetic field, J. Comput. Phys. 228 (2009) 2604–2615.
[24] R.M. Santilli, Foundations of Theoretical Mechanics I, Springer-Verlag, New York, 1978.
[25] R.M. Santilli, Foundations of Theoretical Mechanics II, Springer-Verlag, New York, 1983.
[26] Y. Sun, Z. Shang, Structure-preserving algorithms for Birkhoffian systems, Phys. Lett. A 336 (2005) 358–369.
[27] M. Suzuki, General theory of higher-order decomposition of exponential operators and symplectic integrators, Phys. Lett. A 165 (1992) 387–395.